Cement & Concrete Composites 34 (2012) 306–312

Contents lists available at SciVerse ScienceDirect

Cement & Concrete Composites

journal homepage: www.elsevier.com/locate/cemconcomp

Ethyl silicate for surface treatment of concrete – Part I: Pozzolanic effect of ethyl silicate

Franco Sandrolini [1], Elisa Franzoni *, Barbara Pigino [2]

Dipartimento di Ingegneria Civile, Ambientale e dei Materiali, Facoltà di Ingegneria, Università di Bologna, Via Terracini 28, 40131 Bologna, Italy

ARTICLE INFO

Article history:
Received 11 July 2011
Received in revised form 6 December 2011
Accepted 12 December 2011
Available online 20 December 2011

Keywords:
Consolidation
Protection
Ethyl silicate
Calcium hydroxide
Pozzolanic behaviour
Architectural restoration
Cement-based materials

ABSTRACT

Despite the widespread use of ethyl silicate for stone consolidation, the investigation of its reactivity with the different supports is still in progress. In this paper, the pozzolanic behaviour of ethyl silicate is investigated, by means of experimental mixtures of commercial ethyl silicate and slaked lime, and the occurrence of C–S–H formation is shown. The ability of ethyl silicate to penetrate in porous building materials as a liquid solution and, only after curing, to give rise to a pozzolanic material encourages the application of ethyl silicate for the consolidation and protection of reinforced concrete, as well as for the consolidation of modern cement-based mortars having artistic value (Art Nouveau cement-based mortars, etc.). The pozzolanic effect of ethyl silicate can be exploited also for the formulation of new consolidating materials (e.g. with nanolime).

1. Introduction and research aims

Ancient porous building materials (natural stones, bricks, mortars, etc.) undergo several on-site chemical, physical–mechanical and biological degradation processes [1–5], leading to severe decay forms, such as detachment, solubilisation, black crusts formation and alveolisation. Such degradation may cancel the architectural elements' shape, details and decorations, resulting in the building's overall architectural image loss, and even threatening the structural stability itself. Hence, the restoration practice often requires, after accurate cleaning [6], the application of consolidating products [7], in order to provide the decayed materials with proper cohesion and mechanical performance (i.e., as similar as possible to those of the sound substrate).

Among the consolidants, ethyl silicate (ethyl esther of silicic acid – $Si(OC_2H_5)_4$ or $Si(OEt)_4$ – often referred to as TEOS – tetraethylorthosilicate), a silicon-based consolidant of the alkoxysilanes group, is surely one of the most used in ancient building materials' conservation. Once penetrated into the material pores, ethyl silicate, by means of a classic sol–gel process [8], first undergoes hydrolysis (by water in the pores and water vapour in the atmosphere [9]), forming silanol (with Si–OH groups, Fig. 1a) and ethanol, which evaporates without any damaging residues in the material; afterwards, by a dehydration/condensation process, silica gel precipitates inside the material's porous microstructure.

In stones containing silicate phases (e.g. sandstones), silica gel also reacts with the hydroxyl groups present onto the pores surface (Fig. 1b), thus partially restoring the natural binder lost during the weathering processes and reconnecting loosened mineral grains, with a consolidating effect and an appreciable increase in the material mechanical strength [9]. On the contrary, in carbonate stones [10] silica gel just precipitates inside the pores, resulting in a simple filling of pores and a weak, merely physical, bond with the substrate [11].

The widespread use of ethyl silicate is due to its chemical inorganic–organic formulation, small monomer sizes and low viscosity [8], which provide (i) a high penetration depth; (ii) a good compatibility with the support (due to the inorganic nature of its final product, i.e. silica); (iii) an excellent stability in outdoor environment (UV radiation, pollution, etc.), unlike many polymeric consolidants [12]; (iv) an only partial reduction of open porosity and, hence, of water vapour permeability [13]; (v) volatile by-products (i.e., ethanol and water), surely not damaging the stone; (vi) no abrupt interruption between the impregnated and the untreated zones [13]. These are the reasons why it is well accepted by most of Italian Superintendence, whose main concern is compatibility and durability of consolidants.

However, despite the widespread use of ethyl silicate, three main drawbacks have been identified for it:

* Corresponding author. Tel.: +39 051 2090329; fax: +39 051 2090322.
E-mail addresses: franco.sandrolini@mail.ing.unibo.it (F. Sandrolini), elisa.franzoni@unibo.it (E. Franzoni), barbara.pigino2@unibo.it (B. Pigino).
[1] Tel.: +39 051 2090339; fax +39 051 2090340.
[2] Tel.: +39 051 2090361; fax +39 051 2090322.

0958-9465/$ - see front matter © 2011 Elsevier Ltd. All rights reserved.
doi:10.1016/j.cemconcomp.2011.12.003

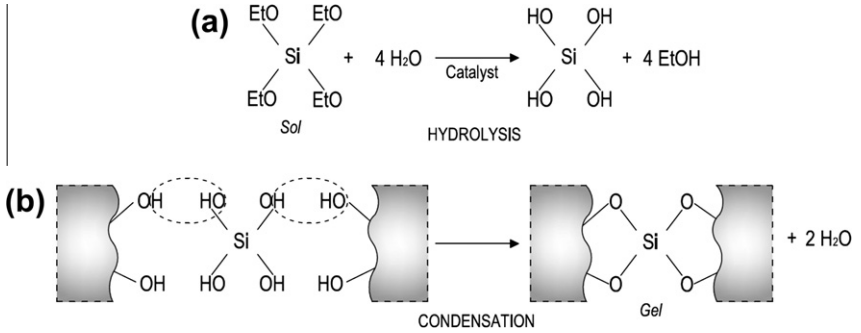

Fig. 1. Reaction scheme for ethyl silicate [Et = C_2H_5]: (a) hydrolysis reaction, with silanol and ethanol formation; (b) simplified condensation reaction in presence of –OH groups in the stone.

- Its poor consolidating effectiveness in carbonate stones [9,14]. A strong research effort is currently focused on solving this problem by means of: preliminary calcareous stone treatment with ammonium hydrogen tartrate, forming calcium tartrate with calcite, able to condense with ethyl silicate and create Si–O–C links [15]; or coupling agents addition [16].
- Its slow reactivity, significantly improved by means of catalyst addition [7].
- Its significant cracking during shrinkage and drying [14]. However, encouraging improvements in this direction are currently in progress, by means of nanoparticles addition [17], additives introduction [18] or hybridization with hydroxyl-terminated polydimethylsiloxane [9].

Hence, many "shadow-zones" still exist to completely assess the on-site performance of ethyl silicate. In particular, the investigation of the interactions between consolidant and support is of great interest [19], as it plays a key role in the treatment efficacy [10], and some efforts have already been undertaken in this direction, e.g. investigating TEOS reactivity with quartz and calcite supports [19].

In this paper, an experimental system has been developed for investigating the reactivity between ethyl silicate and calcium hydroxide, in order to asses TEOS's pozzolanic behaviour and formation of hydrated calcium silicates (C–S–H); the performance of ethyl silicate for the treatment of hardened concrete will be discussed in the second part of the paper [20]. The pozzolanic behaviour of fine (micro- or nano-sized) silica powders is of great interest for the production of more durable mortars and concrete [21–25]. In the present paper, the pozzolanic effect of TEOS is particularly attractive as this material can penetrate in the existing porous building materials due to its liquid solution nature and, only after curing, give rise to the pozzolanic reaction. Hence it might be used for the treatment of $Ca(OH)_2$-rich substrates, such as reinforced concrete [20], cement-based historic mortars and conglomerates (the decorative elements of Art Nouveau architectural heritage, etc.), or lime-based mortars and plasters (possibly not fully carbonated). Moreover, modification of TEOS consolidants by nanolime [26–28] addition may be explored.

As suggested by other authors [19], the reactivity between TEOS and a substrate may be investigated by mixtures of the consolidant with the relevant powdered stone, in order to simplify the actual support-consolidant system, usually very complex due to the heterogeneous composition and microstructure of buildings materials. Therefore, the use of mixtures of ethyl silicate and slaked lime has been envisaged as suitable for the investigation of the pozzolanic behaviour of TEOS.

Table 1
Main chemical–physical characteristics of the ethyl silicate used [29].

Active ingredient	Tetra-ethyl-ortho-silicate
Content of active ingredient [wt.%]	75
Solvent	White spirit
Viscosity [cp]	4.9 (20 °C)
Density [kg/l]	0.98 (20 °C)
Dry residual [wt.%]	Minimum 35
Boiling point [°C]	145–200
Appearance	Colourless liquid
Solubility in water	Insoluble
Risk phrases (directive 2001/59/EC)	Ethyl silicate: Xn; R 20; R 36/37; R 10
	Solvent: Xn; R 65; R 10
	Catalyst: Xn + N; R 48/22; R 36/38; R 50/53
Safety phrases (directive 2001/59/EC)	S 7/8; S 16; S 20/21; S 24–26; S 36–39; S 47; S 61

2. Materials and specimens

2.1. Materials

A commercially available ethyl silicate, henceforth named *E* (Estel 1000, CTS, Italy, Table 1), and a commercially available slaked lime, henceforth named *C* (Cari, Italy) were used. Prior to the samples preparation, *E* was concentrated by evaporation of the solvent under a ventilated hood (weight reduction 20%), in order to promote a better interaction between *E* and *C*.

2.2. Mixtures and specimens

The slaked lime and the concentrated ethyl silicate were used for preparing the experimental mixtures reported in Table 2: the mixtures were prepared in a UNI EN 196-1 Hobart mixer (10′ stirring at speed 1), were poured into 100 × 100 × 10 mm moulds and were cured in both laboratory environment, at $T = 22 \pm 1$ °C and RH = 30–50% (M1-series samples in Table 2), and humid atmosphere, at $T = 22 \pm 1$ °C and RH > 96% (M2-series samples in Table 2), for 2 and 12 months. As a matter of fact, air relative humidity is known to strongly influence the hardening time of TEOS [7].

3. Methods

The particle size distribution of the slaked lime was determined by a laser particle size analyzer (Malvern Mastersizer 2000 equipped with a Hydro 2000 MU): before measurement, the sample was dispersed by stirring (2500 rpm) in a 0.025% tetramethylammonium-hydrate solution and then exposed to ultrasonics (10 μm) for 1 min. The carbonate content of *C* was determined by the Dietrich–Frühling method.

Table 2
Mixtures formulations.

Sample	Ethyl silicate [wt.%]	Slaked lime [wt.%]	Curing conditions	Thermal treatment
E	100	–	Air (RH = 30–50%)	–
C	–	100	Air (RH = 30–50%)	–
M1	50	50	Air (RH = 30–50%)	–
M2	50	50	RH > 96%	–
M1-800-30	50	50	Air (RH = 30–50%)	800 °C, 30 min
M1-800-60	50	50	Air (RH = 30–50%)	800 °C, 60 min
M1-800-120	50	50	Air (RH = 30–50%)	800 °C, 120 min
M1-800-240	50	50	Air (RH = 30–50%)	800 °C, 240 min
M2-800-30	50	50	RH > 96%	800 °C, 30 min
M2-800-60	50	50	RH > 96%	800 °C, 60 min
M2-800-120	50	50	RH > 96%	800 °C, 120 min
M2-800-240	50	50	RH > 96%	800 °C, 240 min

The mixtures microstructure was investigated, after curing, by mercury intrusion porosimetry (Porosimeter 2000 Carlo Erba, equipped with Fisons Macropore Unit 120; maximum pressure 2000 bar; cylindrical calculation model; contact angle mercury/material = 141.3°). Water absorption at environmental pressure (WA%) was determined after drying at 100 ± 5 °C to constant weight (M_d) and subsequent water immersion to constant weight (M_{wet}), as $WA\% = 100\cdot(M_{wet}-M_d)/M_d$. The bulk volume (and hence bulk density, ρ) was determined on the same water-saturated samples by the hydrostatic weighing method.

After grinding to a fineness <0.075 mm, the mixtures were characterised by powder X-ray diffraction (XRD) in a Philips Diffractometer PW1840 operating at 40 kV/20 mA (Cu Kα radiation with $\lambda = 1.54184$ Å; scan range $2\theta = 5–60°$; step size $2\theta = 0.020°$; scan speed $2\theta/s = 0.020$; time for step 1.0 s; Philips Analytical PC-PDF Diffraction Software and PDF-2 Reference Database). The carbonate content of the ground mixture was determined by the same Dietrich–Frühling method quoted above.

The powdered mixtures were investigated by thermal-gravimetric analysis (TGA Q50, TA Instruments; operating conditions: from 30 °C to 900 °C at 30 °C/min in nitrogen atmosphere, gas flow 40 ml/min).

Fourier-Transform Infrared Spectroscopy equipped with a Universal Attenuated Total Reflectance Sampling Accessory, FTIR-ATR (Perkin Elmer Spectrum One) was used, putting the samples in direct contact with the ATR crystal, over the wave number range of 650–4000 cm^{-1}.

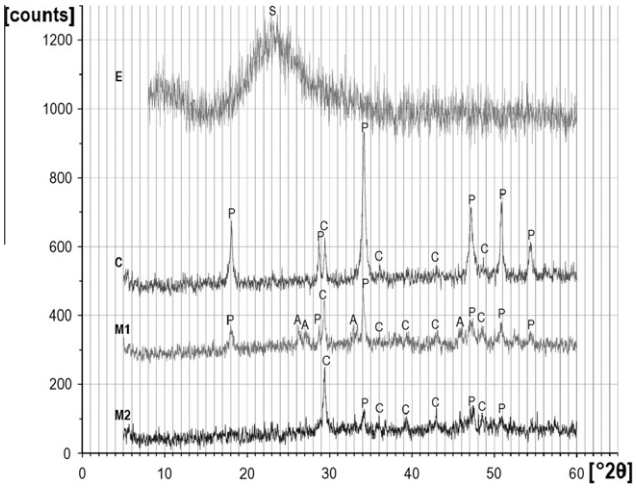

Fig. 2. XRD plots of *E*, M1 and M2 samples at 2 months, along with that of the starting *C* sample [*A* = aragonite (PDF N. 41-1475); *C* = calcite (PDF N. 5-586); *P* = portlandite (PDF N.4-733); *S* = amorphous silica].

Moreover, some cured samples were milled and thermally treated in an oven at 800 °C (for 30, 60, 120 and 240 min, Table 2). This thermal treatment was performed in order to promote the formation of higher ordered structures from C–S–H and, hence, for a better detection of them. On such thermally treated mixtures, the same XRD analysis quoted above was carried out.

4. Results and discussion

4.1. Starting materials

The slaked lime showed an average grain size of 8.9 μm ($d_{10\%} = 2.7$ μm, $d_{90\%} = 34.2$ μm) and a calcium carbonate content of 28.7%, which is in the normal range for slaked lime currently employed in construction.

4.2. Experimental mixtures

The XRD plots of *E*, M1 and M2 samples after a curing period of 2 months and 1 year respectively, together with that of the starting

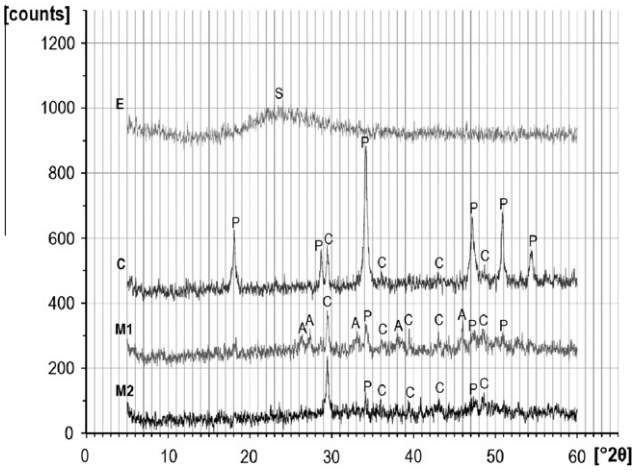

Fig. 3. XRD plots of *E*, M1 and M2 samples at 1 year, along with that of the starting *C* sample [*A* = aragonite (PDF N. 41-1475); C = calcite (PDF N. 5-586); *P* = portlandite (PDF N.4-733); *S* = amorphous silica].

Table 3
$CaCO_3$ amount in the experimental mixtures [wt.%].

Mixture	2 Months curing	1 Year curing
M1	44.2	52.7
M2	28.7	31.2

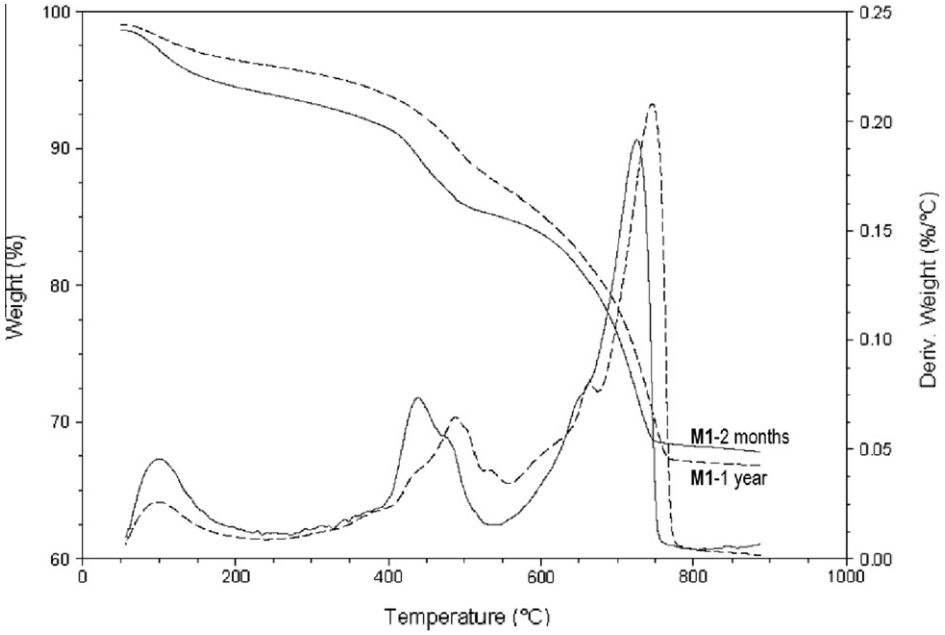

Fig. 4. TGA results for M1 mixtures at 2 months and 1 year.

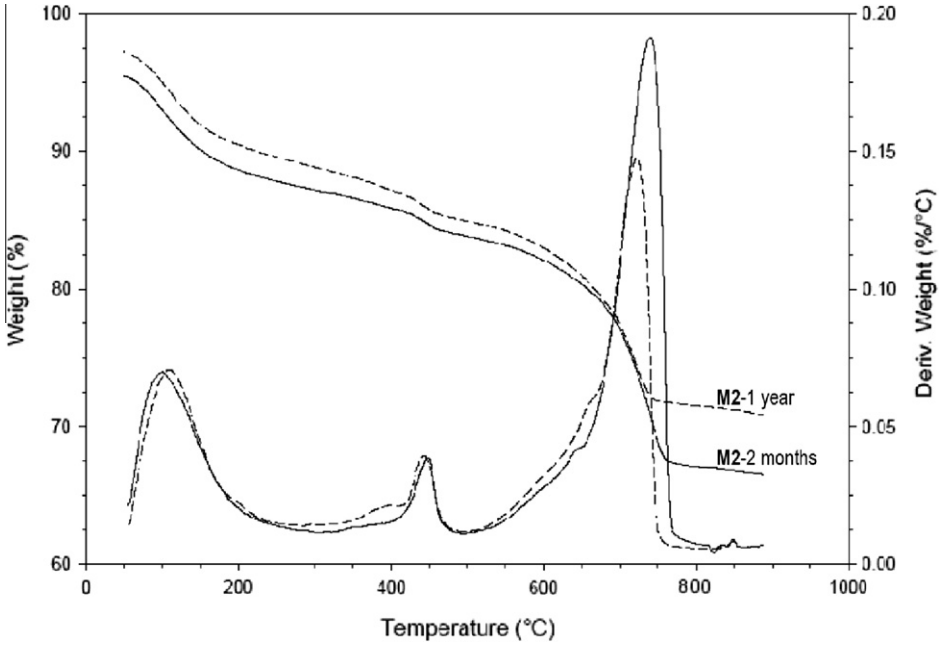

Fig. 5. TGA results for M2 mixtures at 2 months and 1 year.

C sample, are reported in Figs. 2 and 3, while the relevant $CaCO_3$ amounts of M1 and M2 are reported in Table 3. *E* sample simply shows a smoothed peak corresponding to amorphous silica gel [30], as expected, while the slaked lime exhibits dominant calcium hydroxide (portlandite) peaks and minor calcium carbonate (calcite) peaks. After 2 months room air curing (Fig. 2), the M1 sample shows only small $Ca(OH)_2$ peaks and a calcite content of 44 wt.% (Table 3); after 2 month curing at RH > 96%, $Ca(OH)_2$ peaks have almost disappeared in the M2 sample and a calcite amount of only 29 wt.% was detected (Table 3): this suggests the formation of some reaction products between calcium hydroxide and ethyl silicate, scarcely detectable by XRD due to their barely ordered structure (moreover, the main peak of hydrated calcium silicate – e.g., PDF N. 33-306 – if present, would be overlapped by the calcite peaks). After 1 year (Fig. 3 and Table 3), the sample's composition has not significantly changed for the moist-atmosphere cured samples (M2), but has changed for the air cured ones (M1): in particular, $Ca(OH)_2$ has slightly decreased, $CaCO_3$ has increased (from 44% to 53% in Table 3) and low but clear aragonite peaks have appeared in the XRD diagram. This is compatible with the formation of C–S–H (hydrated calcium silicates) in the mixture: as a matter of fact, C–S–H undergoes, for long curing in presence of low relative humidity, some "carbonation" process, leading to the formation of silica gel and aragonite [31–33].

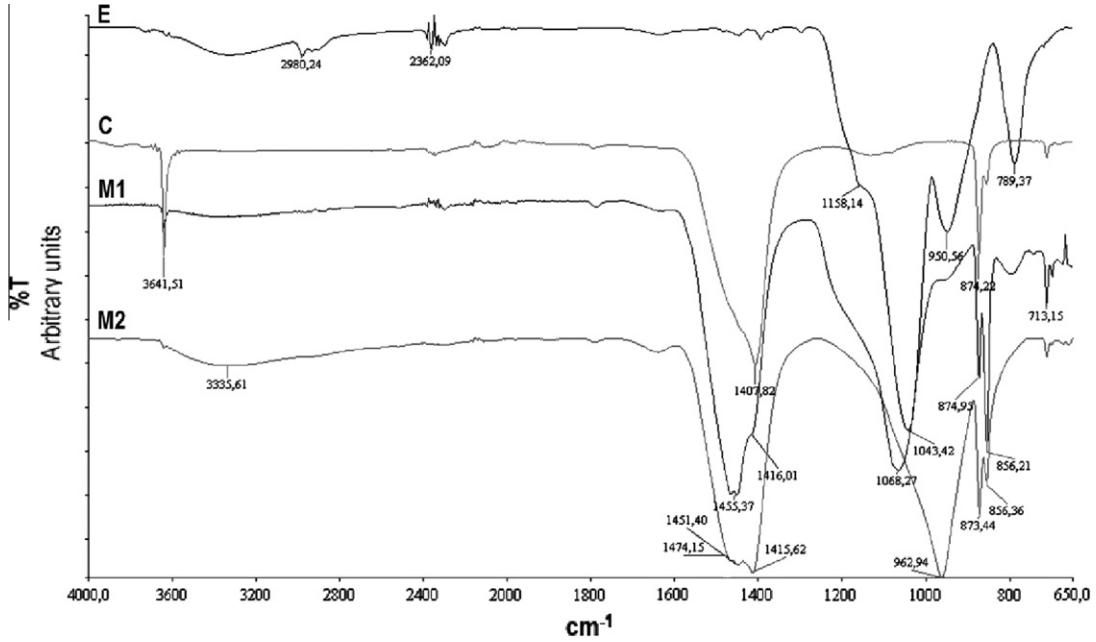

Fig. 6. FTIR-ATR spectra for *E*, M1 and M2 at 1 year, along with the starting slaked lime.

Table 4
Assignment to the main peaks observed in the FTIR-ATR spectra.

Wave number [cm^{-1}]	Functional bond	Assigned to	Refs.
790	Si–O–Si	SiO_2	[36]
880–850	CO	$CaCO_3$	[37]
950	Si–OH	Silanol groups	[36]
970–960	Si–O	C–S–H	[31,36]
1070–1040	Si–O–Si	SiO_2	[36]
1100	Si–O–C	Ethyl silicate	[38]
1470–1410	CO	$CaCO_3$	[31,37]
2980	–CH	Solvent	[39]
2800–3700	Si–OH	Silanol groups	[40]
3640	O–H	$Ca(OH)_2$	[31,37,41]

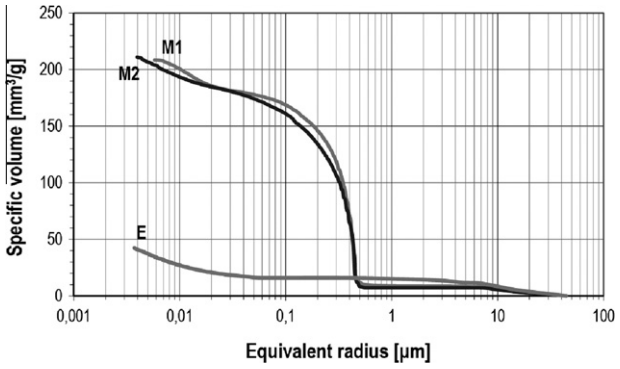

Fig. 7. Pore size distribution of *E*, M1 and M2 at 1 year.

The TGA results are reported in Figs. 4 and 5 for M1 and M2 mixtures respectively and weight losses are observed at the following characteristic temperatures:

- about 100 °C, water and residual solvent evaporation (see also Table 1);
- about 450 °C, dehydration of calcium hydroxide [31];
- about 480 °C, dehydration of silica gel (assessed by TGA on cured *E* sample);

Table 5
Microstructural characteristics of the mixtures at 1 year.

Mixture	Pores mean radius [μm]	Bulk density [g/cm^3]	Total open porosity [%]	Water absorption [%]
M1	0.45	1.52	31.67	24.97
M2	0.47	1.42	31.96	32.36
E	0.006	1.55	6.57	–

- about 650 °C, dehydration of C–S–H [34,35];
- 680–750 °C, decarbonation of calcite/aragonite.

The weight loss at about 650 °C is ascribable to C–S–H compounds [34,35], hence corroborating the hypothesis of pozzolanic behaviour of ethyl silicate. The weight loss at about 480 °C, due to silica gel, occurs only in the M1 sample, where some presence of silica gel is expected not only from the condensation of TEOS, but also as a consequence of the carbonation of C–S–H in dry atmosphere, as mentioned above [31–33]; such weight loss is absent in the M2 sample, suggesting a complete reaction between silica gel and calcium hydroxide.

The FTIR-ATR spectra of the 1-year-cured *E*, M1 and M2 mixtures are reported in Fig. 6, together with that of the starting slaked lime, while the relevant chemical compounds are listed in Table 4. Bands corresponding to silica gel are clearly distinguishable in the *E* spectrum, together with those of silanol groups, residual solvent and residual not hydrolysed ethyl silicate. In the M1 spectrum, the vibration bands of silica gel still appear, but are less defined, while in the M2 spectrum they are not detectable. It is noteworthy that, in the M2 spectrum, the characteristic peak at 962 cm^{-1} confirms the presence of C–S–H. Such a C–S–H peak is barely detectable in the M1 spectrum, probably because of a lower amount of C–S–H in the mixture (possibly also due to the carbonation process described above).

The pore size distributions of *E*, M1 and M2 samples after 1 year curing are reported in Fig. 7, while their microstructural features (bulk density and water absorption) are reported in Table 5: both M1 and M2 samples are quite similar in terms of their pores' mean size and open porosity. The porosity is quite high (about 32%), due

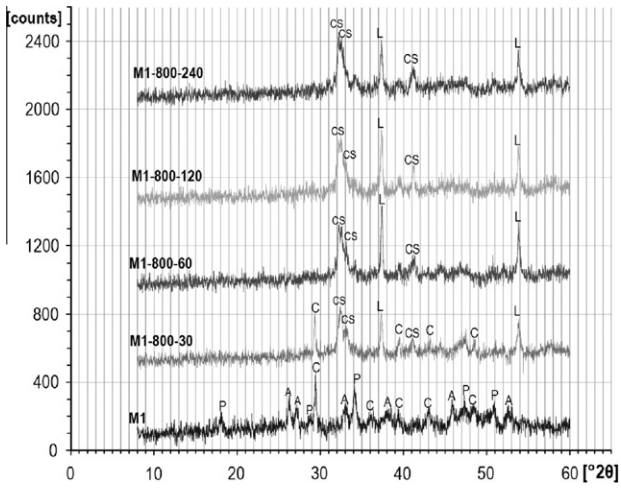

Fig. 8. XRD diagrams of the thermally treated M1 samples. [*A* = aragonite (PDF N. 41-1475); *C* = calcite (PDF N. 5-586); C_2S = dicalcium silicate (PDF N. 33-302); *L* = CaO (PDF N. 37-1497); *P* = portlandite (PDF N. 4-733)].

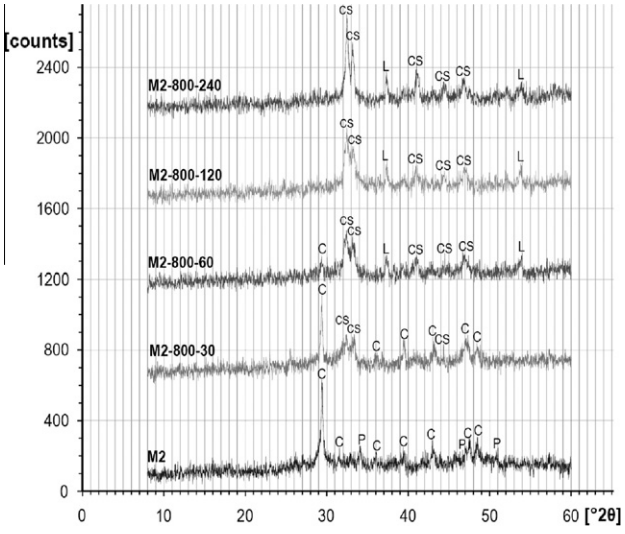

Fig. 9. XRD diagrams of the thermally treated M2 samples. [*C* = calcite (PDF N. 5-586); C_2S = dicalcium silicate (PDF N. 33-302); *L* = CaO (PDF N. 37-1497); *P* = portlandite (PDF N. 4-733)].

to the conspicuous solvent amount in the starting TEOS solution. In fact, although the solvent content was reduced by means of the concentration procedure described above in Section 2.1, a certain amount was nonetheless necessary in order to obtain a suitable fresh-state workability for the mixtures. The cured *E* sample shows a low and nano-sized porosity (Fig. 7 and Table 5), caused by the sol–gel hardening process.

4.3. Thermally treated experimental mixtures

For a better identification of the reaction products between calcium hydrate and ethyl silicate, the 1-year-cured experimental mixtures were thermally treated. The treatment at 800 °C produced the modifications shown in Figs. 8 and 9: in both the mixtures, the heat treatment promoted the formation of C_2S, coming from the dehydration of C–S–H, and CaO, coming from the dehydration of calcium hydroxide and the decarbonation of $CaCO_3$ (i.e., calcite in M2; calcite and aragonite in M1).

5. Conclusions

The pozzolanic behaviour of ethyl silicate has been ascertained by means of experimental mixtures of commercial ethyl silicate and slaked lime. The evidences of the formation of C–S–H compounds are multiple, as given by XRD, FTIR and TGA analyses performed on both simply cured and thermally treated samples. The influence of the environmental relative humidity on the pozzolanic reaction has been evaluated as well.

The exploitation of the pozzolanic behaviour of ethyl silicate for the surface treatment of concrete will be discussed in the second part of the paper [20].

Acknowledgements

CTS srl is gratefully acknowledged for the TEOS supply. Thanks to Dr. Paola Marchese and Dr. Michaela Vannini for their support in the FTIR analyses.

References

[1] Alice VT, Thomas RP. Sandstone weathering: a century of research and innovation. Geomorphology 2005;67(1–2):229–53.
[2] Camuffo D. Physical weathering of stones. Sci Total Environ 1995;167(1–3):1–14.
[3] Theoulakis P, Moropoulou A. Microstructural and mechanical parameters determining the susceptibility of porous building stones to salt decay. Constr Build Mater 1997;11(1):65–71.
[4] Warscheid T, Braams J. Biodeterioration of stone: a review. Int Biodeter Biodegr 2000;46(4):343–68.
[5] Sandrolini F, Franzoni E, Cuppini G. Predictive diagnostics for decayed ashlars substitution in architectural restoration in Malta. Mater Eng 2000;11(3):323–37.
[6] Moropoulou A, Tsiourva Th, Bisbikou K, Tsantila V, Biscontin G, Longega G, et al. Evaluation of cleaning procedures on the facades of the bank of Greece historical building in the center of Athens. Build Environ 2002;37:753–60.
[7] Amoroso GG, Fassina V. Stone decay and conservation: atmospheric pollution, cleaning, consolidation and protection. Amsterdam: Elsevier; 1983 [p. 370].
[8] Mosquera MJ, De los Santos DM, Montes A, Valdez-Castro L. New nanomaterials for consolidating stone. Langmuir 2008;24:2772–8.
[9] Zárraga R, Cervantes J, Salazar-Hernandez C, Wheeler G. Effect of the addition of hydroxyl-terminated polydimethylsiloxane to TEOS-based stone consolidants. J Cult Heritage 2010;11:138–44.
[10] Dei L, Salvadori B. Nanotechnology in cultural heritage conservation: nanometric slaked lime saves architectonic and artistic surfaces from decay. J Cult Heritage 2006;7:110–5.
[11] Scherer GW, Wheeler GS. Silicate consolidants for stone. Key Eng Mater 2009;39:1–25.
[12] Lazzarini L, Laurenzi Tabasso M. Il Restauro della pietra. Torino: Utet Scienze Tecniche; 2010.
[13] Delgado-Rodrigues J. Consolidation of decayed stones. A delicated problem with few practical solutions. In: Lourenço PB, Roca P, editors. Proceedings of the 3rd international seminar on historical constructions, Universidade do Minho, Guimarães; 2001. p. 3–14.
[14] Maravelaki-Kalaitzaki P et al. A comparative study of porous limestones treated with silicon-based strengthening agents. Prog Org Coat 2008;62:49–60.
[15] Slavid IO, Weiss NR. Method for protecting and consolidating calcareous materials. US patent 6296905. 2 October; 2001.
[16] Wheeler G et al. Evaluation of alkoxysilane coupling agents in the consolidation of limestone. In: Proceedings of the 9th international congress on deterioration and conservation of stone. Amsterdam: Elsevier Science Pub.; 2000. p. 541–5.
[17] Miliani C, Velo-Simpson ML, Scherer GW. Particle-modified consolidants: a study on the effect of particles on sol–gel properties and consolidation effectiveness. J Cult Heritage 2007;8:1–6.
[18] Kim EK, Won J, Do J-Y, Kim SD, Kang YS. Effects of silica nanoparticle and GPTMS addition on TEOS-based stone consolidants. J Cult Heritage 2009;10:214–21.
[19] Zendri E, Biscontin G, Nardini I, Riato S. Characterization and reactivity of silicatic consolidants. Constr Build Mater 2007;21:1098–106.
[20] Pigino B, Leemann A, Franzoni E, Lura P. Ethyl silicate for surface treatment of concrete. Part II: characteristics and performance. Cem Concr Compos 2012;34:313–21.
[21] Pacheco-Torgal F, Jalali S. Nanotechnology: advantages and drawbacks in the field of construction and building materials. Constr Build Mater 2011;25:582–90.
[22] Dai JG, Akira Y, Wittmann FH, Yokota H, Zhang P. Water repellent surface impregnation for extension of service life of reinforced concrete structures in marine environments: the role of cracks. Cem Concr Compos 2010;32:101–9.

[23] Senff L et al. Mortars with nano-SiO_2 and micro-SiO_2 investigated by experimental design. Constr Build Mater 2010;24:1432–7.
[24] Gaitero JJ, Campillo I, Guerriero A. Reduction of the calcium leaching rate of cement paste by addition of silica nanoparticles. Cem Concr Res 2008;38:1112–8.
[25] Moropoulou A, Cakmak A, Labropoulos KC, Van Grieken R, Torfs K. Accelerated microstructural evolution of a calcium–silicate–hydrate (C–S–H) phase in pozzolanic pastes using fine siliceous sources: comparison with historic pozzolanic mortars. Cem Concr Res 2004:341–6.
[26] Ambrosi M et al. Colloidal particles of Ca(OH)2: properties and applications to restoration of frescoes. Langmuir 2001;17:4251–5.
[27] Daniele V, Taglieri G, Quaresima R. The nanolimes in cultural heritage conservation: characterisation and analysis of the carbonatation process. J Cult Heritage 2008;9:294–301.
[28] Daniele V et al. Risultati preliminari di trattamenti conservativi a base di nanocalce su arenarie emiliane. In: Biscontin G, editor. Il consolidamento degli apparati architettonici e decorativi: conoscenze, orientamenti, esperienze. Atti del XXIII Convegno Internazionale Bressanone 10–13 luglio 2007. Padova: Libreria Progetto Editore; 2007. p. 367–74.
[29] CTS Srl. Altavilla Vicentina (VI). Italy: technical and safety data sheets of ''Estel Line'' ethyl silicate.
[30] Singh D, Kumar R, Kumar A, Rai KN. Synthesis and characterization of rice husk silica, silica–carbon composite and H_3PO_4 activated silica. Cerâmica 2008;54:203–12.
[31] Villain G, Thiery M, Platret G. Measurement methods of carbonation profiles in concrete: thermogravimetry, chemical analysis and gammadensimetry. Cem Concr Res 2007;37:1182–92.
[32] Thiery M, Villain G, Dangla P, Platret G. Investigation of the carbonation front shape on cementitious materials: effects of the chemical kinetics. Cem Concr Res 2007;37:1047–58.
[33] Slegers PA, Rouxhet PG. Carbonation of the hydration products of tricalcium silicate. Cem Concr Res 1976;6:381–8.
[34] Bažant ZP, Kaplan MF. Concrete at high temperatures. Harlow: Longman; 1996 [p. 20 and 28].
[35] Moropoulou A, Bakolas A, Bisbikou K. Characterization of ancient, byzantine and later historic mortars by thermal and X-ray diffraction techniques. Thermochim Acta 1995;269–270:779–95.
[36] Rubio F, Rubio J, Oteo JL. A DSC study of the drying process of TEOS derived wet silica gels. Thermochim Acta 1997;307:51–6.
[37] García Lodeiro I, Macphee DE, Palomo A, Fernández-Jiménez A. Effect of alkalis on fresh C–S–H gels FTIR analysis. Cem Concr Res 2009;39:147–53.
[38] Ioele M, Santamaria U, Tiano P. Studio comparativo di silicati di etile commerciali e sperimentali a confronto con microemulsioni acriliche per il consolidamento di matrici carbonatiche fortemente decoese. In: Proceedings of International Congress The silicates in conservative treatments: texts, improvements and evaluations of consolidating performance, 13–15 Febbraio, Villa Gualino, Torino. Torino: Associazione Villa dell'Arte; 2002. p. 71–82.
[39] Croveri P, Appolonia L. Il silicato di etile a confronto con consolidanti fluorurati: distribuzione all'interno di substrati porosi e cinetiche di reazione. In: Proceedings of international congress the silicates in conservative treatments: texts, improvements and evaluations of consolidating performance, 13–15 Febbraio, Villa Gualino, Torino. Torino: Associazione Villa dell'Arte; 2002. p. 83–92.
[40] Weinstock BA, Yang H, Griffiths PR. Determination of the adsorption rates of aldehydes on bare and aminopropylsilyl-modified silica gels by polynomial fitting of ultra-rapid-scanning FT-IR. Vib Spectrosc 2004;35:145–52.
[41] Lavat AE, Trezza MA, Poggi M. Characterization of ceramic roof tile wastes as pozzolanic admixture. Waste Manage 2009;29:1666–74.